

Gas-Phase Polymerization of Butadiene. Data Acquisition using Minireactor Technology and Particle Modeling

M. Bartke, A. Wartmann, K.-H. Reichert

Institut für Technische Chemie, Technische Universität Berlin, D-10623 Berlin, Germany

Received 23 October 2000; accepted 10 December 2001

ABSTRACT: Minireactor technology has been used for kinetic studies on polymerization kinetics, phase equilibrium, and mass transfer on a very small scale. There is a nonlinear influence of temperature and pressure on the polymerization rate. The phase equilibrium can be described by a Flory–Huggins approach, with a temperature-dependent interaction parameter. The diffusion coefficient seems to be slightly pressure dependent, and the temperature dependence can be described with an Arrhenius equation. A simple formal kinetic scheme with formation of active sites, chain propagation, chain transfer to cocatalyst, and deactivation of active sites has been applied. This kinetic scheme was implemented in two different models; they are, a particle model taking into account mass transfer and a simple

chemical model with no mass transfer. In principle, both models describe the experimental results for rate and molecular weight distribution equally well, with rate constants of the same magnitude. Molecular weight distributions calculated by the chemical model are narrower. However, the chemical model gives no explanation for the experimental observed rate dependence on catalyst particle size. With increasing catalyst activity, the differences between both models become more significant and the particle model becomes more and more important. © 2002 Wiley Periodicals, Inc. *J Appl Polym Sci* 87: 270–279, 2003

Key words: gas-phase polymerization; butadiene; minireactor; kinetics; molecular weight distribution; modeling

INTRODUCTION

In general, supported catalysts are used for gas-phase polymerization reactions. For process design, the catalysts have to be characterized in terms of reaction engineering. Many physical and chemical processes (reaction kinetics, phase equilibrium, mass and heat transfer, catalysts fragmentation) occur simultaneously. As a result, many of the corresponding parameters cannot be determined independent of each other. Therefore, these parameters have to be fixed by model-based analysis and fit to an integral quantity being measured. Suitable integral variables for gas-phase polymerization are the polymerization rate and the molecular weight distribution (MWD).

In this work, specially designed minireactors for fast screening of catalysts and measurement of the activity of catalysts are presented. Results for gas-phase polymerization of butadiene with a Ziegler-type catalyst based on neodymium are shown. Phase equilibrium and mass transfer of butadiene in butadiene rubber are also studied. Finally, two models, a reaction/diffusion particle model and a chemical model, are developed to describe the kinetics and MWD of the polymerization. The differences are discussed.

POLYMERIZATION EXPERIMENTS

In general, stirred tank reactors with volumes of 1–5 L are used for kinetic studies on gas-phase polymerization processes. Often, bed materials have to be used to prevent sticky polymer particles from agglomeration.¹ Preparing and running of these experiments is a time-consuming procedure. A simple measuring system was developed for fast catalyst screening and kinetic measurements of gas-phase polymerization reactions. The experiments were run on a very small scale, so only 2–3 mg of catalyst are needed for one experiment.

Pressure drop minireactor

The setup of the measuring system can be seen in Figure 1. The basic concept is a very compact reactor, which can be introduced into a glove box. This compactness allows one to limit catalyst handling to the glove box only. The reactor (Figure 2) consists of three parts: the reaction chamber, a glass view port to close the chamber, and thermostating jacket. First the reaction chamber and the view port are cleaned and introduced into the glove box, where the reactor is charged with catalyst (~2 mg). Then, the mounted minireactor is connected to the monomer supply. Inert gas is removed from the reactor with a rotary vane vacuum pump, and then the reaction is started with influx of monomer.

Two kinds of experiments can be run in this reactor. In a screening experiment, several different catalysts

Correspondence to: K.-H. Reichert.

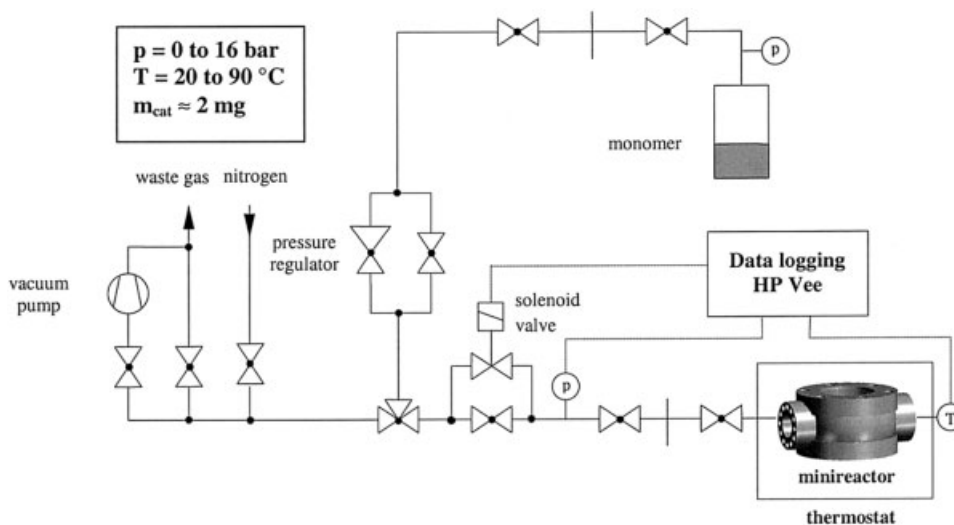


Figure 1 Setup of minireactor for gas phase polymerization.

can be qualitatively tested simultaneously in only one experiment. Therefore, the different catalysts are filled in a special screening plate (Figure 3) with different segments. When an active catalyst has been identified, a quantitative kinetic experiment with only this catalyst can be carried out.

Because the reactor is equipped with a glass view port, the polymer formation can be followed visually. More detailed information about single particle kinetics and start-up of polymerization can be obtained from digital images taken during the course of polymerization.¹

The monomer consumption during polymerization is determined by pressure drop measurements in the range of some millibars (Figure 4). The upper limit of the pressure drop is set with a mechanical pressure controller. When the upper limit is reached, the solenoid valve closes and the reactor is cut off from the monomer supply. Because of monomer reaction, monomer is consumed and the pressure decreases. When the lower limit is reached, the solenoid valve opens and the next pressure drop can be run. The

slope of the pressure drop is a measurement of the reaction rate.

The pressure drops are operated and analyzed automatically with a computer program based on HP Vee® software. The software determines the slope (dp/dt , where p is pressure and t is time) of each pressure drop via a linear correlation fit. This linearization takes place over a small period of time (minutes) compared with the duration of the experiment (hours) and is a known technique in control applications ('linearization at the operating point'). The linear fit is always within the noise of the pressure gauge, which means that the error of the linearization is smaller than the measuring error. With the determined pressure drop (dp/dt), the mass flow of consumed monomer (\dot{m}_M) is calculated using the ideal gas law:

$$\dot{m}_M = \frac{M_M V_R}{RT} \frac{dp}{dt} \quad (1)$$

where M_M denotes the molecular weight of the monomer, V_R denotes the reactor volume, R the universal gas constant, and T is the reaction temperature.

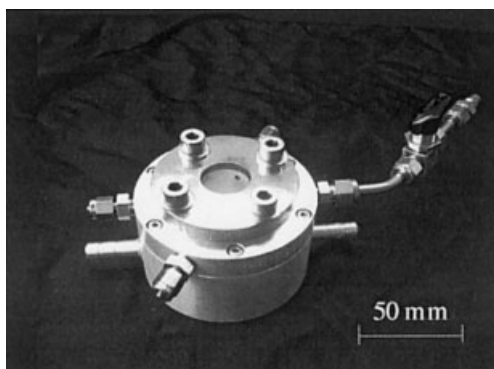


Figure 2 Mounted minireactor.

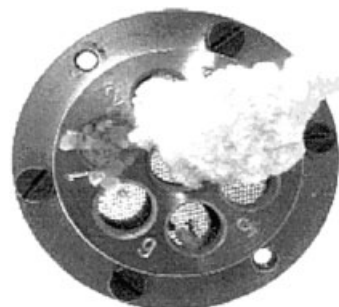


Figure 3 Screening plate for seven different catalysts.

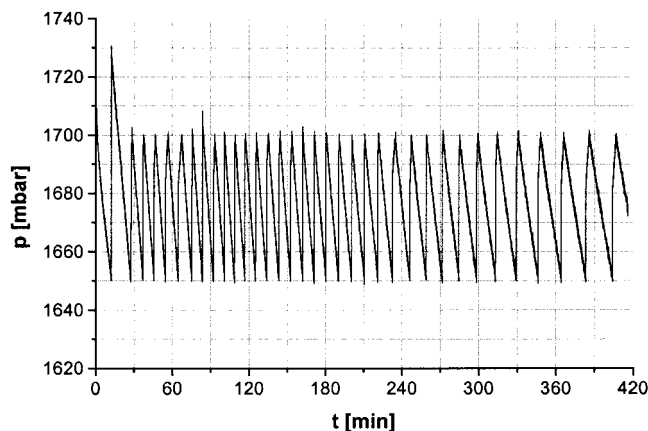


Figure 4 Pressure drop profiles during polymerization.

The sensitivity of the measurement is limited by the signal noise of the pressure gauge. For the pressure gauge used, one can estimate that the pressure drop should be >5 mbar in 3 min. Because of the small reaction volume of ~ 50 cm³, this pressure drop is equal to a mass flow of ~ 180 μ g/min or a volume flow of 0.08 mL/min (298 K, 1013 mbar). The sensitivity of the minireactor device is therefore in the range of most sensitive flow meters commercially available. The rate is calculated online from the mass flow and the amount of used catalyst:

$$\text{rate} = \frac{\dot{m}_M}{n_{Me}^0} = 3.6 \frac{M_M V_R}{n_{Me}^0 RT} \frac{dp}{dt} \left[\frac{\text{kg}_{BR}}{\text{mol}_{Me} \cdot \text{h}} \right] \quad (2)$$

where n_{Me}^0 denotes the moles of active component used in the experiment. The factor 3.6 in eq. 2 results from a unit conversion from g/s to kg/h.

Experiments can be run up to 90°C using water as a thermostating agent and a pressure of 16 bars. Recently, the same setup has been used for gas-phase polymerization of ethylene with a supported single-site catalyst.²

Reproducibility

The main problem of running experimental studies on gas-phase polymerization on a small scale is the reproducibility of the measurements. Equipment should be made of only materials that are resistant to gas diffusion, such as stainless steel or metallic gaskets.

Also, the procedure for cleaning the device, the handling of the catalysts, and especially the quality of the monomer are critical factors affecting reproducibility. The monomer is cleaned in columns with mol-sieve and aluminum oxide just before entering the reactor.

The achieved reproducibility of the gas-phase polymerization can be seen in Figure 5. Plotted are experimental rate–time characteristics at different condi-

tions. The rate [$\text{kg}_{BR}/(\text{mol}_{Nd} \cdot \text{h})$] is defined as quantity of polymer (kg) produced in one hour per amount of neodymium (mol). The experiments were run during a period of 14 months.

Temperature dependence

The temperature dependence of the process is complex. In general, reaction rate and diffusion increase with temperature, whereas the solubility of monomer in polymer decreases with increasing temperature, resulting in a nonlinear temperature dependence of the rate (see Figure 5). The maximum rate, ~ 1200 $\text{kg}_{BR}/(\text{mol}_{Nd} \cdot \text{h})$, is almost the same at different temperatures but the kinetic characteristics differ with respect to temperature. Higher temperatures lead to faster activation and deactivation periods.

Pressure dependence

The pressure dependence of overall reaction rate can also be seen in Figure 5. Plotted are rate–time curves at 50°C and 1.0, 1.675, and 2.0 bars of monomer pressure. There is a strong pressure dependence of the rate. An increase of pressure leads to faster activation periods and to considerable higher rate levels. The maximum rate at 2.0 bars monomer pressure is ~ 1600 $\text{kg}_{BR}/(\text{mol}_{Nd} \cdot \text{h})$, which is about three times the maximum rate at 1.0 bar monomer pressure and same temperature. Reasons for the nonlinear pressure dependence can be the nonlinear phase equilibrium, the reaction rates, and the catalyst fragmentation process.

Influence of catalyst particle size

In a mass transfer limited system, one should observe a dependence of the overall reaction rate with respect to catalyst particle size. Smaller particles have a higher specific interface and the diffusion lengths are shorter than in bigger particles. This size difference leads to higher reaction rates for smaller particles, which is in good agreement with experimental evidence and can be seen in Figure 6, where the reaction rates of two sieved fractions of catalyst particles in the ranges 100–200 and 300–400 μ m are plotted. Different reaction rates for smaller and bigger particles can also be a result of different loadings with the active component (e.g., due to uneven impregnation). However, in this case, the slope of the rate–time characteristic should not change for different particle sizes as they do in Figure 6. Therefore the results shown in Figure 6 are a strong indication that mass transfer resistances are important.

PHASE EQUILIBRIUM AND MASS TRANSFER

Phase equilibrium and mass transfer studies are necessary for determination of monomer concentration at

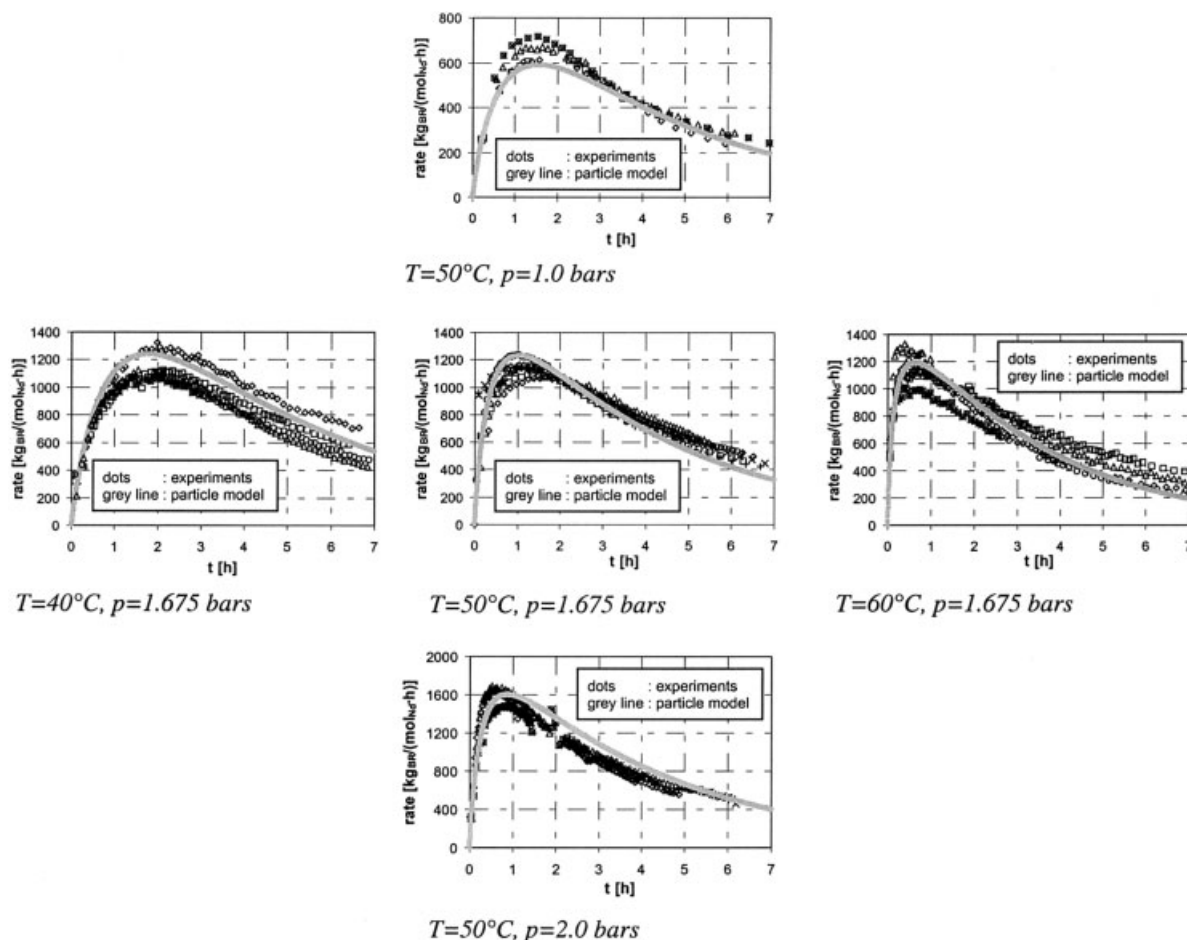


Figure 5 Rate-time plots of gas-phase polymerization under different conditions.

the locus of active sites. These experiments were carried out in a microbalance reactor using sieved polymer particles (gas phase product) of defined particle size.

Microbalance reactor

The microbalance reactor was originally built by Garmatter.³ Some further improvements were made by

Baumann and Bartke.⁴ The setup can be seen in Figure 7.

It is also possible to run polymerization experiments in the microbalance reactor, but in this study it is used for sorption experiments only. Sieved polymer particles are filled onto a scale inside the measuring cham-

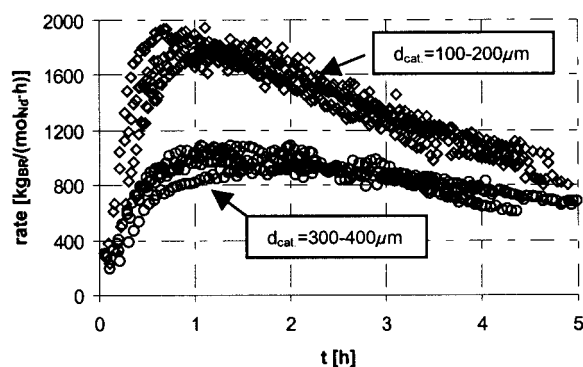


Figure 6 Influence of catalyst particle size on reaction rate at $p = 1.675$ bars and $T = 50^\circ\text{C}$.

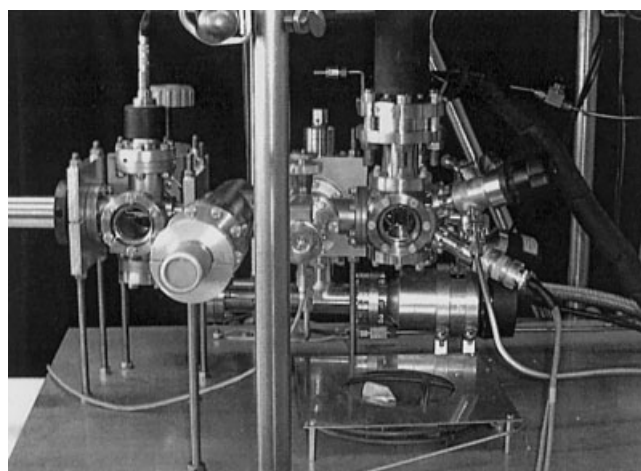


Figure 7 Microbalance reactor for sorption experiments.

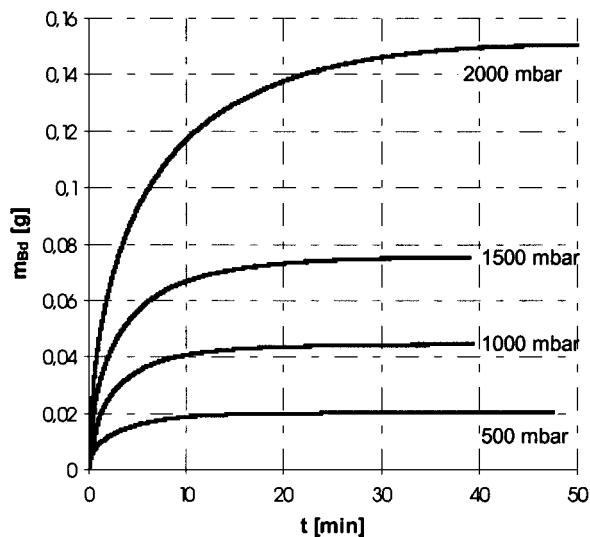


Figure 8 Sorption curves butadiene in polybutadiene at room temperature and different pressures.

ber of the microbalance reactor. The measuring chamber can be seen on the right side of Figure 7. The loading of the scale is transferred without contact to a microbalance, which is standing above the chamber, with a commercially available magnetic suspension coupling (Rubotherm Company, Bochum, Germany). The balance has a sensitivity of $10 \mu\text{g}$ and is connected to a personal computer for data acquisition. The microbalance reactor is equipped with a pressure controller and electrical heating system for temperature control. Experiments can be run in this case up to 2 bars pressure and 90°C .

The sorption experiments are started by addition of monomer. The increase of weight with sorption time is registered. It is necessary to use a compensation for the influence of buoyancy-force to get correct results.

Some curves for sorption of butadiene in butadiene rubber at room temperature can be seen in Figure 8.

Phase equilibrium

The concentration of butadiene at equilibrium can be calculated from the sorbed monomer mass at steady state and the mass of the polymer sample used. In Figure 9, equilibrium concentrations of butadiene in polybutadiene at various conditions are shown (symbols). The lines represent equilibrium calculations using the Flory-Huggins equation and a temperature-dependent interaction parameter. At 50°C , the interaction parameter, χ , is 0.46. The temperature dependence can be described with an Arrhenius equation and an activation energy of -4000 J/mol . These results are in good agreement with the results in the literature.^{3,5}

Mass transfer

Mass transfer in polymerizing particles is a widely discussed topic in research of polyolefins. For porous

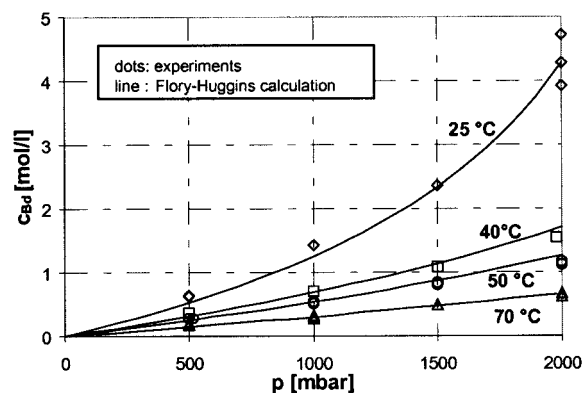


Figure 9 Phase equilibrium butadiene in polybutadiene particles.

polymer particles, it is more and more accepted that in addition to diffusion, convective transport or permeation plays an important role.^{6,7} However, with decreasing porosity of the particles, the influence of convective mass-transfer will decrease more and more. For very compact, nonporous particles, such as polybutadiene particles of gas-phase polymerization, diffusion is the major transport mechanism and convection can be neglected. The corresponding effective diffusion coefficients can be calculated directly by fitting the analytical solution⁸ (eq. 3) of the transient diffusion equation for a sphere to the experimental sorption curves:

$$\frac{m(t)}{m_{\text{equilibrium}}} = 1 - \frac{6}{\pi^2} \sum_{n=1}^{\infty} \frac{\exp(-D_M n^2 \pi^2 t / r_{\text{particle}}^2)}{n^2} \quad (3)$$

where $m(t)$ denotes the actual sorbed butadiene mass, $m_{\text{equilibrium}}$ is the sorbed mass at equilibrium, D_M is the effective diffusion coefficient of butadiene in polybutadiene, and r_{particle} is the polymer particle radius.

In Figure 10, these diffusion coefficients are shown

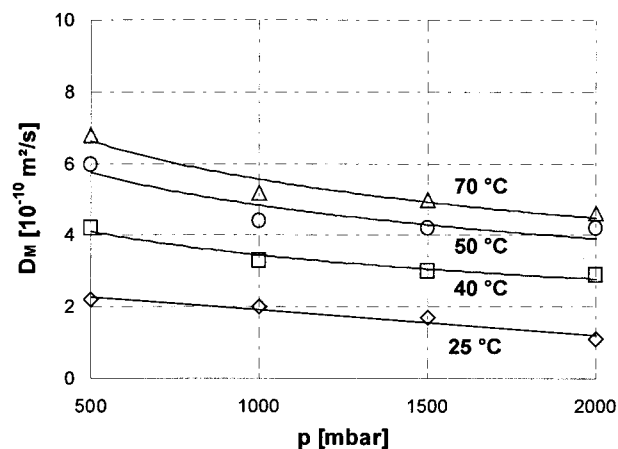


Figure 10 Effective diffusion coefficients for butadiene in polybutadiene particles under various conditions.

for various pressures and temperatures. The diffusion coefficients at constant temperatures are slightly pressure dependent (nonideal diffusion). Considering averages for the diffusion coefficients at constant temperature, the temperature dependence of the averaged effective diffusion coefficients can be described with an Arrhenius equation and an activation energy of 17400 J/mol.

MOLECULAR WEIGHT DISTRIBUTION OF GAS PHASE POLYMERS

For experimental determination of MWD via size exclusion chromatography, a dissolved polymer sample is required. Unfortunately, polybutadiene made by gas-phase polymerization is soluble in tetrahydrofuran (THF) at room temperature only up to 30 to 70 wt %. Because of this bad solubility, the experimental results vary in a broad range, as shown in Figure 11. Plotted are number- and weight average of the MWD for polymerization experiments at 1.675 bars monomer pressure and 50°C temperature with respect to reaction time together with corresponding simulation results (line). MWDs for short, middle, and long reaction times at same conditions can be seen in Figure 12.

MODELING

The reaction takes place in the polymer particles formed. Hence, these particles have to be considered as a kind of microreactor of the system. A lot of effort has been put in the last decades in particle modeling. Starting with very simple morphological assumptions (e.g., core-shell model⁸), more and more detailed models have been developed taking account for mass and heat transfer, particle morphologies (polymeric flow

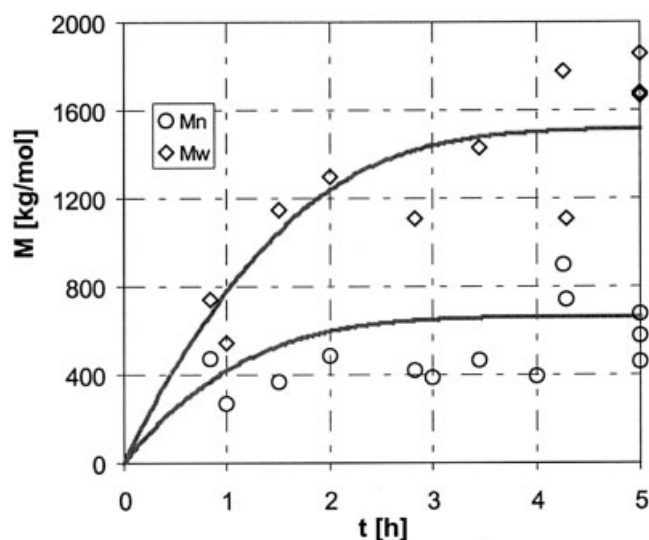
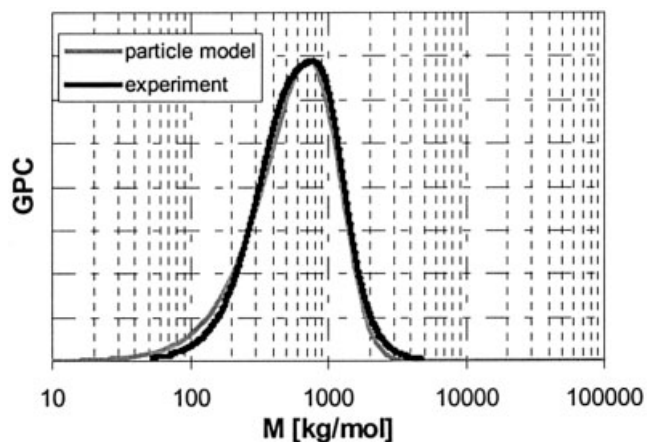
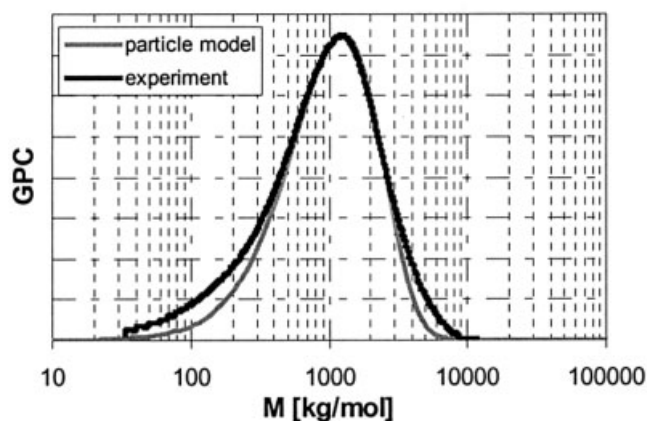


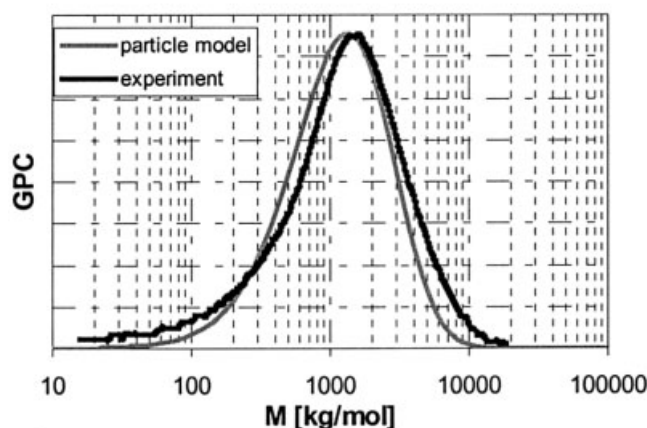
Figure 11 Number and weight average molecular weights for experimental runs at 1.675 bar and 50°C.



50 min reaction time



120 min. reaction time



320 min reaction time

Figure 12 Molecular weight distributions at different reaction times.

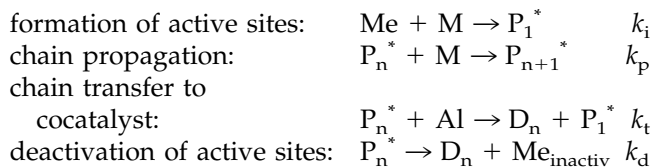
model,⁹ multigrain model^{10,11}) and catalyst fragmentation.^{12,13} For polyolefins, multigrain models^{10,11} are widely used. These models predict polymer particle

porosities in the range of catalyst porosities. However, in gas-phase polymerization of butadiene, very compact, nonporous particles are formed. Therefore, the quasi-homogeneous polymeric flow model is used in this case.

Particle model

The active sites are assumed to be evenly distributed in the catalysts particle. First, the polymerization takes place on the inner and outer surface of the catalyst particles. The formed polymer causes hydraulic forces in the pores, which lead to brake up of the catalyst. In this model, the fragmentation process itself is not considered; we assume it is not the rate-limiting step. The resulting fragments move outwards embedded in the polymer formed, while monomer is transported via diffusion inside the particle. Additionally, the increase of volume by polymer production leads to a dilution effect. Concentration gradients of monomer and active sites are the consequences. Because of these concentration gradients, different MWD at different radial positions of the particle can occur.

Chemical processes at the catalyst surface can be very complex. In the present case however, a simplified formal kinetic scheme is applied:



where k_i , k_p , k_t , and k_d are the rate constants for the outlined reaction steps. This scheme can be derived from the scheme proposed by Honig et al.¹⁴ for Ziegler–Natta polymerization of butadiene, neglecting formation of byproducts and chain transfer to but-1-ene.

Balancing of the polymerizing particle leads to the following equations:

- The mass balance of monomer:

$$\frac{\partial c_M}{\partial t} = D_M \left(\frac{\partial^2 c_M}{\partial r^2} + \frac{2}{r} \frac{\partial c_M}{\partial r} \right) - k_p c_M c_{P^*_{\text{overall}}} \quad (4)$$

where c_M is the monomer concentration, r is the radial position within the particle, and $c_{P^*_{\text{overall}}}$ is the overall concentration of growing chains.

- The convective flow of polymer outwards:

$$\frac{\partial \dot{V}_P}{\partial r} = 4\pi r^2 \frac{M_M}{\rho_P} k_p c_M c_{P^*_{\text{overall}}} \quad (5)$$

where \dot{V}_P is the convective volume flow of formed polymer inside the particle, M_M denotes the molar weight of monomer, and ρ_P is the polymer density.

- The mass balances of all components distributed within the particle by the convective flow:

$$\frac{\partial c_i}{\partial t} = - \frac{1}{4\pi r^2} \frac{\partial}{\partial r} (c_i \dot{V}_P) + R_i \quad (6)$$

where c_i is the concentration of the species i considered, and R_i is the superposition of all reaction rates involved. For growing chains of chain length n one obtains:

$$\begin{aligned} \frac{\partial c_{P_n^*}}{\partial t} = & - \frac{1}{4\pi r^2} \frac{\partial}{\partial r} (c_{P_n^*} \dot{V}_P) + k_p c_M (c_{P_{n-1}^*} - c_{P_n^*}) \\ & - (k_t c_{Al} + k_d) c_{P_n^*} \quad (7) \end{aligned}$$

where $c_{P_n^*}$ is the concentration of growing chains with chain length n , $c_{P_{n-1}^*}$ is the concentration of growing chains with chain length $n - 1$, and c_{Al} is the concentration of cocatalyst.

For calculation of MWD for each chain length, one equation of the type shown in eq. 7 has to be solved. A very large, coupled system of partial differential equations results. Continuous variable transformation^{14–16} is applied to deal with this problem. The discrete chain length is treated as an continuous variable, and a Taylor-series approximation is applied to express the concentration difference in the propagation term of eq. 7. The following, two-dimensional partial differential equation (eq. 8) results and describes the complete MWD:

$$\begin{aligned} \frac{\partial c_{P^*}(n)}{\partial t} = & - \frac{1}{4\pi r^2} \frac{\partial}{\partial r} (c_{P^*}(n) \dot{V}_P) + k_p c_M \left(\frac{1}{2} \frac{\partial^2 c_{P^*}}{\partial n^2} - \frac{\partial c_{P^*}}{\partial n} \right) \\ & - (k_t c_{Al} + k_d) c_{P^*}(n) \quad (8) \end{aligned}$$

The moles of dead chains are calculated by integration over the whole particle:

$$\frac{dn_D(n)}{dt} = 4\pi \int_0^{r_{\text{max}}} (k_t c_{Al} + k_d) c_{P^*}(n) r^2 dr \quad (9)$$

where $n_D(n)$ is the overall amount of dead chains with chain length n within the particle.

The resulting equations have to be solved together with an energy balance of the particle. This solving is done numerically using a gPROMS (Process Systems Enterprise, London, UK) simulation software package. One problem for numerical solution is the particle growth. The right boundaries of the partial differential equations are moving with reaction time (moving-

boundary-problem). One way to deal with this problem is to normalize the radial position r with respect to particle radius r_{particle} :

$$r_n = \frac{r}{r_{\text{particle}}} = 0 \dots 1 \quad (10)$$

The normalized radius r_n runs from zero to one, and the right boundary is fixed. However, the balancing volumes themselves are moving with time now because the particle radius, r_{particle} , is a function of time. For this grid convection, an additional expression has to be taken into account. For example, for the monomer balance (eq. 4) using normalized radius one obtains:

$$\frac{\partial c_M}{\partial t} = \frac{r_n}{r_{\text{particle}}} \frac{dr_{\text{max}}}{dt} \frac{\partial c_M}{\partial r_n} + \frac{D_M}{r_{\text{particle}}^2} \left(\frac{2}{r_n} \frac{\partial c_M}{\partial r_n} + \frac{\partial^2 c_M}{\partial r_n^2} \right) - k_p c_M c_{P^*} \quad (11)$$

For discrimination, the orthogonal collocation method with evenly distributed grid points in radial direction and the central finite difference method with logarithmic distributed grid points in chain length direction are used.

Chemical model

Alternatively to the complex particle model, a simple chemical model can be discussed. Simplifying the describing equations by neglecting mass transfer and radial concentration gradients leads to a system that can be solved analytically. The monomer concentration remains constant in phase equilibrium to monomer pressure. Using the same kinetic scheme as already outlined, the following balance results for the active metal component:

$$\frac{d}{dt} (c_{\text{Me}} V_{\text{particle}}) = \frac{dn_{\text{Me}}}{dt} = -V_{\text{particle}} k_i c_{\text{Me}} c_M = -k_i c_M n_{\text{Me}} \quad (12)$$

where V_{particle} is the particle volume and n_{Me} is the amount of active metal component in the particle in moles. For calculation of concentrations, the increase of particle volume has to be taken in account. Thus, it is easier to directly calculate moles of interesting species because this quantity only changes by reaction. For an isothermal particle, the analytical solution of eq. 12 is obtained with eq. 13:

$$n_{\text{Me}} = n_{\text{Me}}^0 \cdot \exp(-k_i c_M t) \quad (13)$$

where n_{Me}^0 is the initial amount of active metal component in moles. The balance for overall moles of growing chains was determined as follows:

$$\frac{dn_{P^*}^{\text{overall}}}{dt} = k_i c_M n_{\text{Me}} - k_d n_{P^*}^{\text{overall}} \quad (14)$$

where $n_{P^*}^{\text{overall}}$ is the amount of overall growing chains within the particle in moles.

Assuming that the initial moles of growing chains is equal to zero and using eq. 13, one can derive the analytical solution of eq. 14 (an inhomogeneous, ordinary differential equation of first order) as follows:

$$n_{P^*}^{\text{overall}} = \frac{k_i c_M n_{\text{Me}}^0}{k_d - k_i c_M} [\exp(-k_i c_M t) - \exp(-k_d t)] \quad (15)$$

Thus, the analytical expression for the overall polymerization rate can be obtained as follows:

$$\begin{aligned} \text{rate} &= \frac{M_M k_p c_M n_{P^*}^{\text{overall}}}{n_{\text{Me}}^0} \\ &= 3.6 M_M k_p c_M \frac{k_i c_M}{k_d - k_i c_M} [\exp(-k_i c_M t) \\ &\quad - \exp(-k_d t)] \left[\frac{\text{kg}_{\text{BR}}}{\text{mol}_{\text{Nd}} \cdot \text{h}} \right] \quad (16) \end{aligned}$$

The molecular weight distribution predicted by this chemical model was calculated using Predici (CIT GmbH/Rastede, Germany), a very comfortable modeling tool for polymerization reactions.

Determination of rate constants and discussion

The rate constants can be determined by fitting the simulated quantities to the experimental results. Actually, in this case, the rate constants for formation of active sites, k_i , chain propagation, k_p , and deactivation, k_d , were determined by fitting the simulated overall polymerization rate to the experimental rate-time curves plotted in Figure 5. The rate constant for chain transfer reaction, k_t , does not affect the overall reaction rate. Thus, the transfer velocity can be determined independently of the rate by fitting the simulated MWD to the experimental results. The comparison between experimental (dots) and simulated rates using the particle model (grey lines) can be seen in Figure 5 for various conditions. The comparison of molecular weight and MWD between particle model simulation and experiments can be seen in Figures 11 and 12.

Simulations run with the same set of data and using the chemical model leads to higher rates (Figure 13). This result indicates once more that the measured diffusion coefficients do limit the polymerization rate.

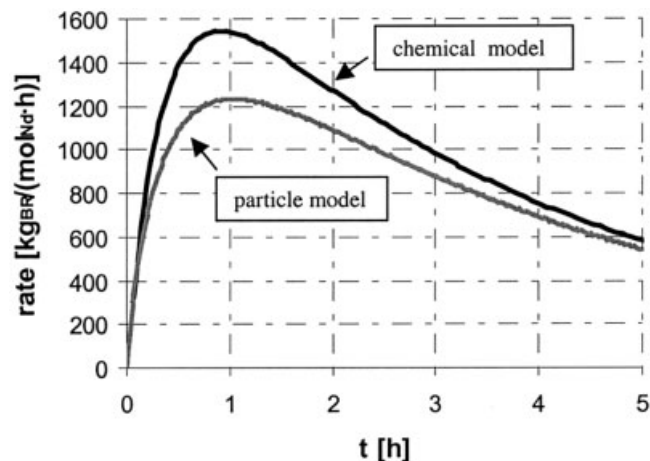


Figure 13 Rate predicted by the particle model and the chemical model using the same set of kinetic data.

However, the experimental results can be described with the chemical model in almost the same quality with another set of rate constants. The comparison of rate constants determined by the two different models can be seen in Table I.

The MWDs predicted by the chemical model are slightly narrower, as evident in Figure 13. Calculated polydispersities are plotted for both models. Unfortunately, the experimental polydispersities are too noisy to give decisive hints as to which model fits better.

It should be noted that the MWD for this system cannot be described with a Schultz–Flory distribution. The living time of polymer chains [$\tau = P_n / (k_p \cdot c_M)$] is in the order of 20 min, so the system has to be considered as a living system with partial deactivation. The MWD starts with a polydispersity of ~ 1.5 and broadens during the course of polymerization to a polydispersity of ~ 2 . This result is typical for living systems with partial deactivation.¹⁸

The polymer samples used for MWD determination were polymerized at the same temperature; hence, it is not possible to give information about the temperature dependence of the transfer rate.

In the chemical model, the rate is not dependent on particle size. Therefore, the results reported earlier cannot be described with this model. Nevertheless, this model can give initial information about rate and MWD with low calculation effort. For catalysts with

higher activity, the diffusion limitation will affect polydispersity much more^{16,17} and the particle model becomes more and more important.

CONCLUSION

For modeling of a gas-phase polymerization process, reliable information about polymerization kinetics, phase equilibrium, and mass transfer in the formed polymer particles is necessary.

Minireactor technology can help to get these data with less effort. It is possible to run reproducible experiments with only 2–3 mg of catalyst per experiment. A kinetic study about gas-phase polymerization of butadiene was carried out, with polymerization experiments run under various conditions.

A microbalance reactor was used for sorption experiments to determine and quantify phase equilibrium and mass transfer. The phase equilibrium can be described with the Flory–Huggins equation and a temperature-dependent interaction parameter.

For modeling, two different models, a particle model taking account for mass transfer and a very simple chemical model without mass transfer, were applied. The rate constants were determined by fitting model predictions for rate and MWD to experimental results.

Simulations run with the same set of data lead to lower reaction rates and to slightly broader MWD with the particle model compared with the chemical model without mass transfer. However, mass transfer seems to be not that important for gas-phase polymerization of butadiene with the catalysts used. Both models are able to describe the experimental results with almost the same quality and with rate constants of same magnitude. The chemical model is not able to explain the experimental observed rate dependence on catalyst particle size.

With increasing catalyst activity, the differences between both models become more significant and a particle model taking into account mass and heat transfer becomes more and more important.

This research project is funded by German Ministry of Education and Research (BMBF) and Bayer AG / Leverkusen, Germany. We are grateful for the granted support. Moreover, we thank Dr. Christian Sommer, Martin Luther Uni-

TABLE I
Fitted Kinetic Data

Rate constant	Particle model		Chemical model	
	50°C	E_A [J/mol]	50°C	E_A [J/mol]
k_i [1/(mol · s)]	$9.05 \cdot 10^{-4}$	100,000	$8.6 \cdot 10^{-4}$	100,000
k_p [1/(mol · s)]	10.55	25,000	7.83	20,000
k_d [1/s]	$7.31 \cdot 10^{-5}$	20,000	$6.46 \cdot 10^{-5}$	25,000
$k_{tr} \cdot c_{Al}$ [1/s]	$6 \cdot 10^{-4}$	—	$6 \cdot 10^{-4}$	—

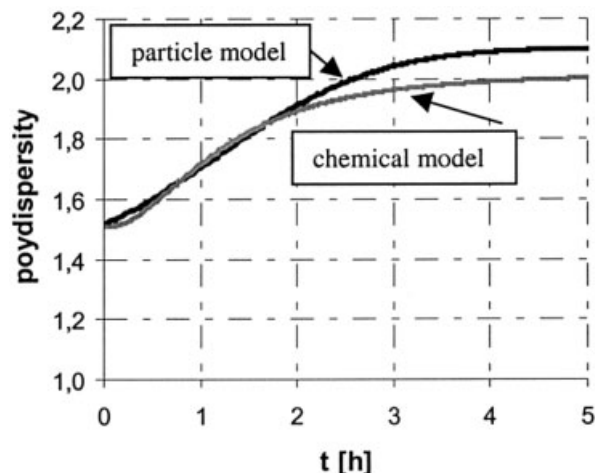


Figure 14 Polydispersity of MWD for particle model and pure chemical model.

versity Halle, Wittenberg, Germany, who measured the MWD.

References

- Zöllner, K.; Reichert, K. -H. *Chem Eng Sci* 2001, 56, 4099.
- Kallio, K.; Wartmann, A.; Reichert, K. -H. *Macromol Rapid Commun* 2001, 22, 1330.
- Garmatter, B. Ph.D. Thesis, TU-Berlin, Berlin, Germany, 1999.
- Bartke, M. Ph.D. Thesis, TU-Berlin, Germany, 2002.
- Spiller, Ch. Ph.D. Thesis, TU-Berlin, Berlin, Germany, 1998.
- Weickert, G.; Meier, G. B.; Pater, J. T. M.; Westerterp, K.R. *Chem Eng Sci* 1999, 54, 3291.
- McKenna, T. F.; Cokljat, D.; Spitz, R.; Schweich, D. *Catalysis Today* 1999, 48, 101.
- Crank, J. *The Mathematics of Diffusion* Oxford University Press: London, 1967.
- Schmeal, W. R.; Street, J. R. *AIChE J* 1971, 17, 1188.
- Floyd, S.; Choi, k.-Y.; Taylor, T. W.; Ray, W. H. *J Appl Polym Sci* 1986, 32, 2935.
- Hutchinson, R. A.; Chen, R. M.; Ray, W. H. *J Appl Polym Sci* 1992, 44, 1389.
- Estenoz, D. A.; Chiovetta, M. G. *Polym Eng Sci* 1996, 36, 2208.
- Przybyla, C.; Weimann, B.; Fink, G. In *Metallorganic Catalysts for Synthesis and Polymerization*; Kaminsky, W., Ed.; Springer: Heidelberg, 2000.
- Honig, J. A. J.; Gloor, P. E.; MacGregor, J. F.; Hamielec, A. E. *J Appl Polym Sci* 1987, 34, 829.
- Zeman, R. J.; Armudson, N. R. *Chem Eng Sci* 1965, 20, 331.
- Bartke, M.; Reichert, K. -H. *Chemie-Ingenier-Technik* 1999, 71, 1310.
- Bartke, M.; Reichert, K. -H. *Chem Eng Technol* 2000, 23, 1062.
- Peebles, Jr., L. H. *Molecular Weight Distributions in Polymers*; John Wiley & Sons: New York, 1971.